INSTITUTE OF PHYSICS PUBLISHING EUROPEAN JOURNAL OF PHYSICS

Eur. J. Phys. **25** (2004) 211–219 PII: S0143-0807(04)66940-6

Measuring the activity of a radioactive source in the classroom

L Peralta

Faculdade de Ciências da Universidade Lisboa and Laboratório de Instrumentação e Partículas, Edificio C8, Campo Grande, 1749-016 Lisboa, Portugal

Received 1 August 2003
Published 6 January 2004
Online at stacks.iop.org/EJP/25/211 (DOI: 10.1088/0143-0807/25/2/008)

Abstract

A standard NaI(Tl) detector can be used in classroom experiments to measure radioactive source activities, once the detector peak efficiencies and geometric acceptances are known. Tables of peak efficiencies for 5.1 cm × 5.1 cm and 7.6 cm × 7.6 cm NaI(Tl) detectors, computed using the GEANT3 Monte Carlo code, are supplied. A Monte Carlo method to compute the geometric acceptance in a general way is also presented.

1. Introduction

The NaI(Tl) gamma detector is a popular detector, which is widely used in undergraduate radiation physics experimental courses. This type of detector can be used to measure radioactive source activities, provided the detector efficiency is known. The activity measurement by an absolute method is a highly pedagogic experiment, where experimental uncertainties must be under control in order to achieve a meaningful result. The main problems can be grouped into three categories: geometric acceptance, detector efficiency, and data analysis. The geometric acceptance should in principle be possible to compute if the source, detector and set-up dimensions are accurately known. For radioactive sources with finite dimensions the problem can became somehow mathematically complex [1]. A Monte Carlo algorithm [2, 3] capable of solving this problem is presented in this work.

Reliable detector intrinsic efficiency data are not usually provided by the manufacturers, leaving the potential user the task of measuring them with calibrated radioactive sources, or to compute them. The first option is not always possible in a teaching laboratory since calibrated radioactive sources are expensive, and several calibrated sources with different energy peaks should be available in order to cover a reasonably wide energy spread. Computation of the detector efficiencies thus looks very attractive. This task can be achieved using one of the presently available radiation Monte Carlo transport codes. In this work the GEANT3 [4] code was used to compute the 5.1 cm × 5.1 cm and 7.6 cm × 7.6 cm NaI(Tl) detector efficiency for several energies and detector–source distances.

Most of the radioactive sources used when teaching radiation physics are solid uncalibrated sealed sources. These are low cost radioactive sources, for which the manufacturers give

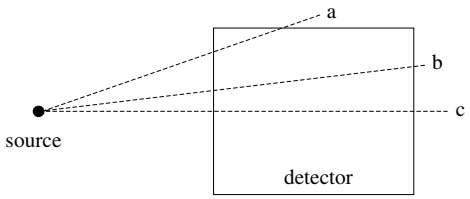

Figure 1. Some directions of gamma photons falling upon the detector from an isotropic radioactive source.

typically [5] a 20% uncertainty on the nominal activity value. For some commonly used radioactive sources a more precise value (of the order of 5%) can be achieved in a careful experiment using the NaI(Tl) detector. How to accomplish this goal is explained in the following sections.

2. The activity measurement

The activity A of a radioactive source with N nuclei of a certain species is defined as the number of decays per unit time

$$A = -\frac{\mathrm{d}N}{\mathrm{d}t} = \lambda N \tag{1}$$

where λ is the decay constant and $\mathrm{d}N$ is the variation of the number of nuclei of that species due only to decays. The experimental activity determination can be made by recording the photon detection rate R (number of photons detected per time unit) due to a particular transition with branching ratio B [6]. If the detection efficiency for these photons is ε, the source activity is given by [1]

$$A = \frac{R}{\varepsilon B}. \tag{2}$$

The total efficiency ε can be factorized into geometric acceptance and detector intrinsic peak efficiency terms [1, 7]. The geometric acceptance is given by the fraction of solid angle defined between the source and the detector, $\Delta\Omega/4\pi$. The detector intrinsic peak efficiency, $\varepsilon_{\mathrm{peak}}$, can be defined as the fraction of photons detected in the full-energy peak relative to the total number of photons incident on the detector. Thus one has for the source activity

$$A = \frac{R}{\varepsilon_{\mathrm{peak}} \frac{\Delta\Omega}{4\pi} B}. \tag{3}$$

3. The peak efficiency

The peak efficiency reflects the number of events detected in the total absorption peak over the total number of events impinging on the detector's window (or wall). It depends on several variables like the gamma energy, the detector characteristics (dimensions, shape, material, etc) and the source's relative placement. The peak efficiency of a system consisting of a source placed inside an infinite detector would be unity, because eventually all energy would be absorbed by the detector. Real systems almost never meet these requirements, but high peak efficiencies can still be obtained. As sketched in figure 1, not all gammas will see the full detector thickness (for example the gamma emitted in the direction a). This effect will be less and less important as the source is placed further away from the detector.

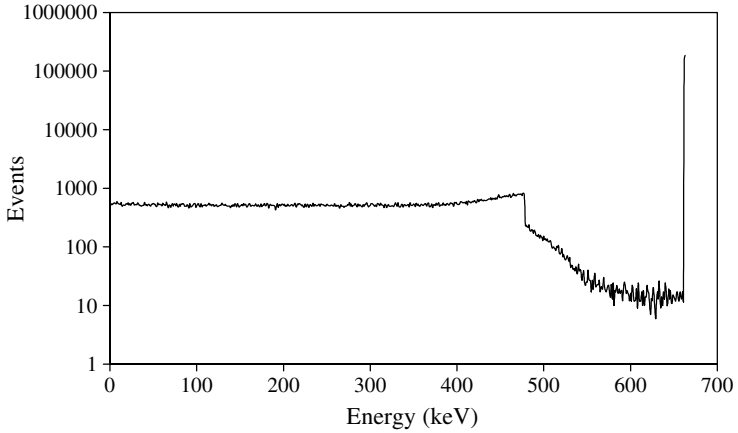

Figure 2. The simulated gamma spectrum of a ^{137}Cs source obtained with a 7.6 cm × 7.6 cm NaI(Tl) crystal.

The best way to evaluate the peak efficiency is by means of a Monte Carlo code that computes the radiation transport through the detector material. Several codes (GEANT3 [4], EGS4 [8] or PENELOPE [9]) can be used for this purpose. As an example, the energy spectrum obtained with GEANT3 for a 662 keV gamma source (^{137}Cs) interacting with a 7.6 cm × 7.6 cm cylindrical NaI(Tl) detector is shown in figure 2. Note the detector resolution, apparently too good, when compared to the typical NaI(Tl) spectrum where a resolution of 7% [10] would be expected. In fact the resolution that can be obtained from this simulated spectrum is the detector intrinsic resolution, due to the energy fluctuations, while the full resolution is affected by the instrumental resolution [1] introduced by the reading device (normally a photomultiplier tube) that reduces the overall resolution.

Based on these energy spectra, the peak efficiency can be computed as the number of events falling in the peak area N_{peak} over the total number of generated events hitting the detector N_{tot}

$$\varepsilon_{\text{peak}} = \frac{N_{\text{peak}}}{N_{\text{tot}}}. \tag{4}$$

The total number of photons N_{tot} is in general greater than the number of photons interacting within the detector, since some of them will pass through the detector without interaction.

Using the GEANT3 code, peak efficiencies have been computed for two of the most commonly used NaI(Tl) detectors in the classroom. They are the 5.1 cm × 5.1 cm and 7.6 cm × 7.6 cm detectors which are manufactured with an aluminium window of 0.05 cm thickness [10]. In tables 1 and 2 the peak efficiencies are presented for the two detectors for different incident photon energies and source–detector distances for an isotropic point source placed along the detector's central axis. For each table entry the number of total generated events N_{tot} is 10^5 for energies in the range 15–1500 keV. The statistical efficiency uncertainty is smaller than 1% in almost all cases, and the relative error can be computed as $1/\sqrt{N_{\text{tot}}\varepsilon_{\text{peak}}}$. This relative uncertainty is adequate for a classroom experiment since, as we shall see, the overall error will be dominated by the geometric acceptance uncertainty. The computed energy values ranging between 15 and 1500 keV cover all common radioactive sources available in the classroom. Since the peak efficiency values have a smooth variation both with energy and distance, the value for a particular set-up may be easily obtained by interpolating the table values. Nevertheless, note the rapid variation of peak efficiency near the 33.2 keV iodine K shell ionization energy.

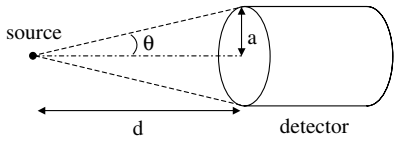

Figure 3. The cylindrical detector solid angle seen by a point source place at a distance d.

Table 1. The peak efficiency of the 5.1 cm × 5.1 cm NaI(Tl) detector.

Energy (keV)	Source–detector distance (cm)						
	0.1	1	3	5	10	20	30
15	0.995	0.988	0.984	0.986	0.990	0.992	0.990
20	0.990	0.978	0.974	0.978	0.985	0.987	0.987
30	0.974	0.961	0.959	0.965	0.974	0.980	0.980
33.2	0.867	0.857	0.863	0.871	0.880	0.883	0.884
35	0.829	0.819	0.826	0.833	0.837	0.843	0.841
40	0.823	0.824	0.834	0.840	0.853	0.857	0.854
50	0.836	0.842	0.857	0.865	0.875	0.882	0.880
60	0.853	0.862	0.874	0.881	0.895	0.901	0.902
70	0.865	0.877	0.882	0.894	0.908	0.916	0.918
80	0.878	0.885	0.886	0.900	0.913	0.925	0.928
90	0.888	0.888	0.882	0.896	0.918	0.928	0.935
100	0.894	0.885	0.875	0.889	0.914	0.931	0.936
150	0.891	0.822	0.796	0.819	0.867	0.906	0.919
200	0.820	0.705	0.683	0.718	0.789	0.847	0.867
300	0.598	0.488	0.478	0.521	0.598	0.668	0.696
400	0.433	0.348	0.346	0.383	0.448	0.509	0.535
500	0.336	0.269	0.264	0.296	0.352	0.398	0.420
600	0.271	0.213	0.214	0.240	0.287	0.327	0.346
700	0.225	0.180	0.182	0.200	0.240	0.276	0.291
800	0.193	0.154	0.154	0.172	0.206	0.241	0.254
900	0.169	0.135	0.136	0.151	0.182	0.210	0.222
1000	0.149	0.119	0.121	0.136	0.164	0.188	0.202
1100	0.136	0.108	0.109	0.121	0.148	0.170	0.179
1200	0.125	0.097	0.098	0.111	0.133	0.154	0.165
1300	0.115	0.089	0.089	0.103	0.123	0.143	0.150
1400	0.105	0.082	0.084	0.093	0.115	0.134	0.139
1500	0.097	0.075	0.077	0.087	0.108	0.125	0.133

4. The geometric acceptance

For an arbitrary detector and isotropic point source the geometric acceptance can be defined as the fraction of solid angle subtended by the detector at the source position

$$\varepsilon_{\text{geo}} = \frac{1}{4\pi}\int \mathrm{d}\Omega = \frac{1}{4\pi}\int_A \frac{\vec{r}\cdot\vec{n}}{|r^3|}\,\mathrm{d}A \tag{5}$$

where $\vec{n}$ is a unitary vector perpendicular to the detector surface at each point and $\vec{r}$ the vector linking the point source to a detector elementary area $\mathrm{d}A$. For an extended source an extra integration must be carried out to cover all source points. For a cylindrical detector with a window of radius a and a point source located in the symmetry axis at a distance d from the detector, the solid angle can be computed as (see figure 3)

$$\Delta\Omega = \int_0^{2\pi}\mathrm{d}\phi\int_{\cos\theta}^{1}\mathrm{d}(\cos\theta') = 2\pi(1-\cos\theta) \tag{6}$$

Table 2. The peak efficiency of the 7.6 cm × 7.6 cm NaI(Tl) detector.

Energy (keV)	Source–detector distance (cm)						
	0.1	1	3	5	10	20	30
15	0.996	0.993	0.989	0.987	0.990	0.991	0.991
20	0.990	0.986	0.980	0.982	0.985	0.987	0.988
30	0.974	0.972	0.967	0.969	0.975	0.980	0.980
33	0.872	0.863	0.869	0.873	0.881	0.884	0.886
35	0.837	0.828	0.828	0.835	0.841	0.844	0.848
40	0.831	0.829	0.838	0.842	0.851	0.857	0.857
50	0.840	0.851	0.861	0.864	0.877	0.880	0.882
60	0.853	0.867	0.879	0.887	0.897	0.903	0.905
70	0.867	0.885	0.894	0.899	0.910	0.917	0.920
80	0.882	0.897	0.899	0.903	0.917	0.926	0.929
90	0.891	0.903	0.903	0.908	0.921	0.933	0.936
100	0.899	0.907	0.902	0.904	0.917	0.934	0.939
150	0.908	0.886	0.841	0.849	0.879	0.911	0.924
200	0.881	0.809	0.756	0.761	0.808	0.864	0.885
300	0.735	0.636	0.578	0.596	0.657	0.726	0.760
400	0.587	0.496	0.451	0.468	0.532	0.600	0.638
500	0.485	0.404	0.364	0.383	0.437	0.503	0.538
600	0.407	0.339	0.308	0.323	0.377	0.436	0.463
700	0.351	0.291	0.267	0.283	0.327	0.382	0.411
800	0.316	0.256	0.239	0.253	0.290	0.338	0.368
900	0.283	0.229	0.211	0.225	0.264	0.310	0.336
1000	0.256	0.210	0.191	0.205	0.239	0.281	0.303
1100	0.236	0.191	0.178	0.190	0.221	0.260	0.280
1200	0.222	0.178	0.161	0.176	0.208	0.244	0.259
1300	0.201	0.168	0.152	0.160	0.191	0.223	0.245
1400	0.186	0.155	0.142	0.153	0.181	0.214	0.229
1500	0.180	0.145	0.131	0.138	0.168	0.202	0.218

where

$$\tan\theta = \frac{a}{d} \qquad \text{and} \qquad \cos\theta = \frac{1}{\sqrt{\tan^2\theta + 1}} = \frac{d}{\sqrt{a^2 + d^2}}$$

and the geometric acceptance is given by

$$\varepsilon_{\text{geo}} = \frac{\Delta\Omega}{4\pi} = \frac{1}{2}\left(1 - \frac{d}{\sqrt{a^2 + d^2}}\right). \tag{7}$$

For other detector or source geometries and placement the evaluation of the solid angle can be rather complicated [1]. As an alternative, the geometric acceptance can be numerically computed using a simple Monte Carlo (MC) algorithm. This method uses random numbers to compute the integral in equation (5). For the sake of simplicity we will assume that both source and detector are cylinders (in practice a common situation), although the devised algorithm can easily be adapted to other geometries. The distance between the source face and the detector window is d and an offset x_{off} between the two axes is assumed (see figure 4). As an extra simplification, the origin of the reference frame is placed at the centre of the source face. Thus the centre of the detector window is placed at the point with coordinates $(x_{\text{off}}, 0, d)$.

The MC algorithm can be set as follows.

(1) Start a counter for the total number of event trials, N_{EV}. Define the total number of events to be accepted in the detector window, N_{ACC}.
(2) Loop on N_{ACC} (i.e., from 1 to N_{ACC}).

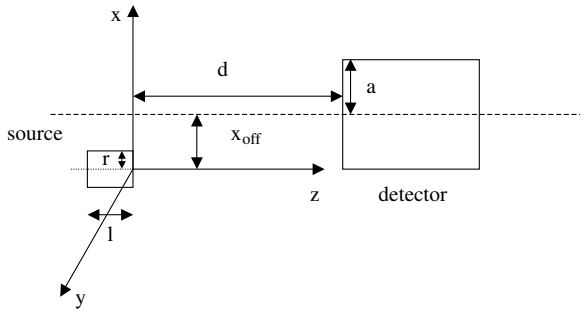

Figure 4. The source–detector arrangement to compute the geometric acceptance by Monte Carlo simulation.

(3) Increment N_{EV} by one and start generating a new emission direction in the forward hemisphere. Using the random number generator, generate two random numbers ξ_1 and ξ_2 uniformly distributed in the interval (0, 1). Compute $\phi = 2\pi\xi_1$ and $\cos(\theta) = \xi_2$, and the direction cosines as $u_x = \sin(\theta)\cos(\phi)$, $u_y = \sin(\theta)\sin(\phi)$ and $u_z = \cos(\theta)$.
(4) Generate a new source emitting point (x_s, y_s, z_s). For a cylindrical source of radius r_s and length l, generate three random numbers ξ_3, ξ_4 and ξ_5 uniformly distributed in the interval (0, 1), compute $\rho^2 = r_s^2\xi_3$, $z_s = -l\xi_4$ and $\varphi = 2\pi\xi_5$. Set $x_s = \rho\cos(\varphi)$, $y_s = \rho\sin(\varphi)$.
(5) Compute the coordinates of the intersection point between the straight line with vector equation $X = X_s + \lambda\vec{u}$ passing through $X_s = (x_s, y_s, z_s)$, with direction $\vec{u} = (u_x, u_y, u_z)$, with the plane passing through the detector window $z = d$. Substituting this last expression in the vector equation, one gets $\lambda = (d - z_s)/u_z$, $x = x_s + \lambda u_x$ and $y = y_s + \lambda u_y$ for the (x, y) coordinates at the detector window plane.
(6) Test if the intersection point lies inside the detector window, i.e., $\sqrt{(x - x_{off})^2 + y^2} \leqslant a$. If not return to step (3) else go to step (2).

Finally, compute the geometric acceptance as $\varepsilon_{geo} = N_{ACC}/2N_{EV}$. Remember that the events were only generated in the forward hemisphere, but a true isotropic source would emit into 4π. The factor 2 in the geometric acceptance expression accounts for this fact.

5. The peak analysis

The final step needed to measure the source activity is to perform the peak analysis and extract the total number of events falling into the peak area. Two main questions have to be addressed at this point: background subtraction and definition of the peak limits. These two topics have some interdependency and must be handled with care. Peak background has three different origins in the case of a NaI(Tl) detector. The first is the electronic noise due to the photomultiplier tube. For typical tubes this is important in the ten to a few hundred kiloelectronvolt range. Second, one has the background due to radioactive sources [1] or cosmic rays. For instance, radon-222 descendants and potassium-40 can usually be seen in the energy spectra. These two contributions to the background can be subtracted from the spectra since their rate can be considered constant for practical purposes. A separate acquisition with no source should then be made. The third peak background has its origin in Compton scattering and the overlap with other peaks. This is an irreducible component and the standard way to subtract it is to fit the peak and background in some user-defined interval using some suitable combination of functions, like Gauss functions for the peaks and a polynomial or exponential function for the background. This procedure requires the use of dedicated fitting software which might not be available to students, complicating the analysis. An alternative approach is, whenever necessary, to fit the background a few channels before and after the peak with

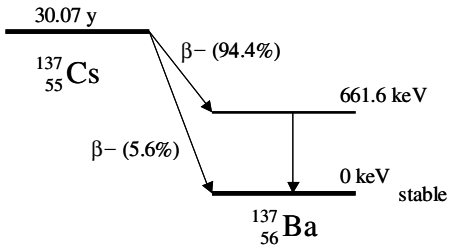

Figure 5. The ^{137}Cs decay scheme (adapted from [13]).

Table 3. The activity results obtained for the calibrated ^{137}Cs source, assuming a crystal of standard dimensions 5.1 cm × 5.1 cm.

Distance (cm)	Peak integral	Geometric acceptance	Peak efficiency	Activity (kBq)
10.42 + 0.095 + 0.05	153 965	0.0139 ± 0.001	0.258 ± 0.002	167.6 ± 6.7
5.61 + 0.095 + 0.05	394 689	0.0429 ± 0.002	0.215 ± 0.001	167.8 ± 6.3

a simple function like a straight line [1] or an exponential, where a standard least squares fit method can be used [7, 11, 12]. Some care must also be taken when choosing the peak limits since this will affect the final peak area, and it is not always clear where to set the limits when peaks overlap. As a general prescription, assuming Gaussian peaks of standard deviation σ, the limits can be set at $\pm 3\sigma$ around the peak centroid, which corresponds to 99.7% of the total peak area.

6. An example of activity measurements with a 5.1 cm × 5.1 cm detector

As an application example we started by measuring the activity of a calibrated ^{137}Cs source held by our laboratory. The source is housed in an aluminium case with 1.9 mm height and its activity on the day was 181.9 kBq. The source was centred with respect to the detector, and two acquisitions where made at two different distances from the detector. The nominal detector dimensions were assumed and for the geometric acceptance evaluation the source case half-height (0.95 mm) and the detector window thickness (0.5 mm) were added to the face-to-face source–detector distance. The background was acquired for a longer time interval than the ^{137}Cs spectra and after rescaling was subtracted from them. The statistical uncertainty introduced by the background subtraction is thus very small (also because the background contribution to the ^{137}Cs peak is small), but still it was taken into account in the final error propagation. Since the 662 keV peak is the highest energy peak in the ^{137}Cs spectrum (see figure 5), there is no need for further background subtraction.

The results obtained for the 662 keV peak (branching ratio $B = 0.851$ [13]) for an acquisition time of 5 min and two source–detector distances are presented in table 3, and the spectra can be seen in figure 6.

For the sake of simplicity only the statistical error on the peak integral has been considered, although this underestimates its value since, for instance, the influence on changing the peak limits is not taken into account. The geometric acceptance errors have been computed assuming a 0.5 mm uncertainty both in the detector radius and source–detector distance. The results in table 3 show a departure from the expected activity value, although they are compatible with that value within the uncertainties.

The geometric acceptance and peak efficiency have been computed assuming standard crystal dimensions, but real crystals are manufactured with tolerances that can reach 2 mm

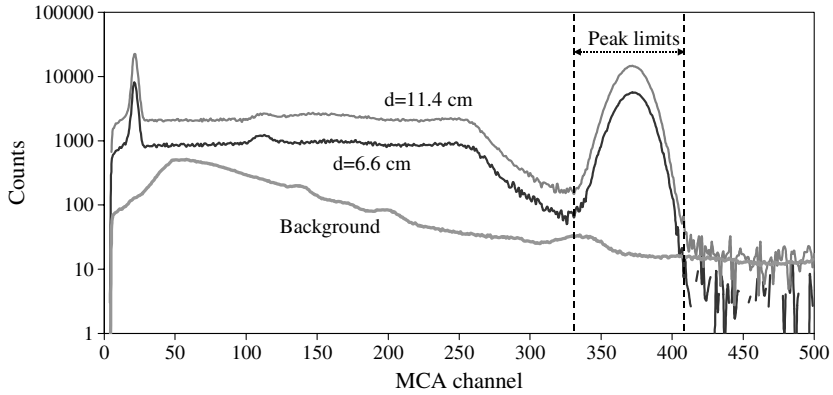

Figure 6. ^{137}Cs gamma spectra obtained with a 5.1 cm × 5.1 cm NaI(Tl) detector at two different source–detector distances (11.4 and 6.6 cm). The dashed lines indicate the used peak limits, for the analysis corresponding to $\pm 3\sigma$ around the peak centroid.

Table 4. The activity results obtained for the calibrated ^{60}Co source for both gamma peaks. The geometric acceptance has been corrected relatively to the standard crystal dimensions, assuming a smaller crystal radius of 2.45 cm.

Energy (keV)	Distance (cm)	Peak integral	Geometric acceptance	Peak efficiency	Activity (kBq)
1173	10.42 + 0.095 + 0.05	3080	0.0129 ± 0.0005	0.137 ± 0.001	5.81 ± 0.26
1332	10.42 + 0.095 + 0.05	2682	0.0129 ± 0.0005	0.120 ± 0.001	5.77 ± 0.26
1173	5.61 + 0.095 + 0.05	7765	0.0399 ± 0.0015	0.114 ± 0.001	5.70 ± 0.22
1332	5.61 + 0.095 + 0.05	6564	0.0399 ± 0.0015	0.010 ± 0.001	5.48 ± 0.22

according to the manufacturer. A difference of 1 mm in the crystal radius would have a small impact on the peak efficiency, but could lead to a significant effect in the geometric acceptance. If one assumes a crystal radius of 2.45 cm, the geometric acceptances will be 0.0129 ± 0.0005 and 0.0399 ± 0.0015, leading to activity values of 181.1 ± 7.4 and 180.0 ± 7.0 kBq, in better agreement with the expected value. In order to test the correctness of the smaller crystal dimensions hypothesis, the activity of a different calibrated source was measured. This time a ^{60}Co source with the same type of aluminium case and an activity of 5.480 kBq on the day was used. The main gamma peaks have energies of 1173 and 1332 keV with branching ratios of 99.9% [13]. The results obtained, again for an acquisition time of 5 min and the same distances as before, are presented in table 4 and are in good agreement with the expected activity value.

7. Conclusion

In this work it has been demonstrated that activity measurements can be performed in the classroom using a standard NaI(Tl) detector. Relative uncertainties of the order of 5% can be attained in such a measurements, much better than the uncertainties provided by common uncalibrated radioactive sources. The primary source of error is the uncertainty in the geometric acceptance, due to dimension tolerances of the crystal. The systematic error can be partially corrected if a calibrated source is available. The geometric acceptance can be tuned by changing the used crystal size, allowing the measured activity to match the calibrated value. The main goal of the present work was to provide peak efficiencies for two common NaI(Tl) detector sizes, and a reliable method to compute geometric acceptances. Peak analysis was kept simple, appropriate to a straightforward classroom application.

References

[1] Knoll G F 2000 *Radiation Detection and Measurement* 3rd edn (New York: Wiley)
[2] Gentle J E 2003 *Random Number Generation and Monte Carlo Methods* (New York: Springer-Verlag)
[3] Press W *et al* 1990 *Numerical Recipes, the Art of Scientific Computing* (Cambridge: Cambridge University Press)
[4] CERN Program Library 1993 *GEANT—Detector Description Simulation Tool (CERN Program Library Long Writeup* W5013*)* (Geneva23: CERN-CH)
[5] CANBERRA data sheets http://www.canberra.com/products/822.asp
[6] Krane K 1988 *Introductory Nuclear Physics* (New York: Wiley)
[7] Leo W R 1987 *Techniques for Nuclear and Particle Physics Experiments* (Berlin: Springer)
[8] Nelson W R, Hirayama H and Rogers D W O 1985 *Stanford Linear Accelerator Report* SLAC-265
[9] Sempau J *et al* 1997 An algorithm for Monte Carlo simulation of coupled electron–photon transport *Nucl. Instrum. Methods* B **132** 337–90
[10] CANBERRA 2003 data sheets *Model 802 Scintillation Detectors* http://www.canberra.com/pdf/Products/Detectors_pdf/2m802.pdf
[11] Cowan G 1998 *Statistical Data Analysis* (Oxford: Clarendon)
[12] Lyons L 1985 *Statistics for Nuclear and Particle Physics* (Cambridge: Cambridge University Press)
[13] Chu S Y F, Ekström L P and Firestone R B 1999 *On-Line Table of Isotopes* http://nucleardata.nuclear.lu.se/nucleardata/toi/